BOX BEHNKEN DESIGN AND DEVELOPMENT OF ROPINIROLE LOADED CHITOSAN NANOPARTICLES FOR INTRANASAL DELIVERY IN PARKINSON'S DISEASE

Christina Das[1], V. Muruganantham[2]*

Article History: **Received: 30.04.2023** **Revised: 26.05.2023** **Accepted: 24.06.2023**

Abstract

Parkinson's disease (PD) is a prevalent neurodegenerative disorder that affects millions of individuals worldwide. This study focuses on the development of Ropinirole loaded chitosan nanoparticles for intranasal delivery, to enhance drug delivery to the brain and improve therapeutic outcomes. Ropinirole is a dopamine agonist used for managing PD symptoms. A Box-Behnken design (BBD) was employed for the optimization of the Ropinirole loaded chitosan nanoparticles. Chitosan, sodium tripolyphosphate (TPP), and Ropinirole were chosen as independent variables. The Ropinirole loaded chitosan nanoparticles evaluated with parameters of particle size, PDI, drug entrapment efficiency, and drug release kinetics. The results revealed the successful formulation of Ropinirole loaded chitosan nanoparticles with desirable physicochemical properties. The FTIR analysis confirmed the compatibility between the drug and excipients. DSC analysis provided insights into the thermal behaviour of the nanoparticles. The developed nanoparticles offer potential advantages for intranasal drug delivery in Parkinson's disease treatment. Intranasal delivery allows direct access to the central nervous system, bypassing the blood-brain barrier and reducing systemic side effects. The sustained release characteristics of the nanoparticles can enhance drug concentration in the brain and reduce dosing frequency. Further studies are warranted to evaluate the efficacy and safety of these Ropinirole loaded chitosan nanoparticles in Parkinson's disease therapy.

Keywords: Ropinirole, chitosan nanoparticle, Parkinson's disease, intranasal delivery, in-vitro drug release, Box Behnken design.

[1]Research Scholar, Vinayaka Mission's Research Foundation, Salem, Tamil Nadu.
[2]*Professor, Vinayaka Mission's College of Pharmacy, Salem, Tamil Nadu

***Corresponding Author:** V. Muruganantham
*Professor, Vinayaka Mission's College of Pharmacy, Salem, Tamil Nadu
Email: svmanand@gmail.com

DOI: 10.48047/ecb/2023.12.si10.004

1.Introduction

Parkinson's disease (PD) is the second-most common neurodegenerative disease in the US, behind Alzheimer's. Over 10 million people have PD, with 4% under 50. Men develop PD 1.5 times more often than women (1).

Ropinirole is a dopamine agonist used to manage Parkinson's disease and restless leg syndrome. It acts by targeting dopamine receptors known as D2 receptors, which are inhibitory neurons that regulate signal transmission (2). By mimicking dopamine's effects, ropinirole compensates for its deficiency and improves signal transmission, leading to a reduction in PD symptoms. It also stimulates D2 and D3 receptors in the basal ganglia, improving motor function (3,4).

Nasal drug delivery may reach the brain. It is needle-free, self-medicating, non-invasive, and requires less dosage than oral administration (5). Various pathways, including systemic, olfactory, and trigeminal, have been identified for drug transport through the nasal cavity (6). The systemic pathway, where the drug enters the systemic circulation through the nasal cavity and crosses the blood-brain barrier (BBB) into the brain; the olfactory pathway, where the drug passes through the olfactory epithelium to reach the olfactory bulb and enter brain tissue or CSF; and the trigeminal pathway, which involves transportation via the trigeminal nerve syst. Due to the nasal cavity being the only site of direct nervous system-environment interaction, technological advances have predicted the rapid and direct delivery of even large and polar medications to the central nervous system (CNS). By extending the subarachnoid space into the nasal cavity, the intranasal route allows drugs to enter the CSF via the olfactory pathway. This method avoids brain damage, invasive implants, and systemic side effects. The hepatic first-pass effect, systemic dilution, off-target drug distribution, higher doses, and more are advantages (7–9).

The rapid clearance of drugs caused by the nasal mucociliary clearance system is a drawback in nose-to-brain drug delivery. As a solution, there has been increased focus on utilizing mucoadhesive polymers, particularly chitosan, in the formulation of nanoparticles (NP) for intranasal delivery (10). A sustained release intranasal nanoparticles were tested for physicochemical properties, sustained release, toxicity, and antiepileptic potential. Fluorescent quantum dots probed brain penetration confirmed promising brain drug delivery efficiency (11). Intranasal chitosan-loaded selegiline nano particles for Parkinson's improved locomotor activity, catalepsy, stride length, brain dopamine, catalase activity, and glutathione content. Intranasal selegiline nanoparticles were better for treating Parkinson's disease than oral ones (12). The results from these studies show that NPs delivered via the nose-to-brain method provided better bio-distribution of the therapeutic agent in the striatum and improved pharmacodynamics as well as provide neuroprotective effects which bypasses the blood-brain barrier (BBB) and enhances drug concentration directly in the brain (10),(13).

Polymer nanoparticles have garnered significant interest as a highly promising drug delivery system for the central nervous system (CNS) due to their ability to target the brain and provide controlled release. Chitosan, derived from chitin through N-acetylation in the presence of hot alkali, is a copolymer consisting of N-acetyl-glucosamine and N-glucosamine units linked by β-(1'4)-glycosidic bonds. Chitosan exhibits excellent bio-compatibility, biodegradability, mucoadhesive, and low toxicity (14).

Ropinirole, selectively stimulate dopamine D2 receptors within the caudate-putamen system in the brain. Due to its low permeability ropinirole has been incorporated within chitosan nanoparticle in this study and that can be administered through intranasal delivery which might have ability to cross BBB and reaching the brain. Where the amount of drug reaching the brain will be greater and produce the desired efficacy. The first pass metabolism, Chemical and enzymatic degradation can be inhibited, and the dosing frequency can be reduced.

2.Materials

Chitosan, sodium tripolyphosphate (TPP) and Ropinirole and were supplied by Loba Chemie, India. All other chemicals were of analytical grade and produced from local vendors.

3.Methodology

Fourier-transform Infrared Spectroscopic analysis:

To investigate the compatibility between the drug samples and excipients, Fourier-transform Infrared Spectroscopic (FTIR) assessment was conducted using Alpha II, Bruker, Germany. The sample powder was dispersed in KBr and drug with a ratio of 1:3 and was prepared by applying 600 Kg/cm2 pressure. The spectrum measurement was attained by powder diffused reflectance on an FT- IR spectrophotometer in wave number 4000cm^{-1} to 400cm^{-1} regions.

Differential scanning calorimetry

The heat difference required to raise the temperature of a sample is determined by the reference temperature in Differential scanning calorimetry (DSC) which is a thermo-analytical procedure using DSC-60, Shimadzu, Japan. DSC technique is widely used to determine the melting point for either pure drugs or mixtures. The samples were pressed using shells made of aluminium. Calorimetric measurements of reference cells are made with an empty shell and calorimetric measurements of sample cells were made with compressing test compounds in the shell. Spectral measurements were collected at a temperature range of 20-310 °C on DSC. DSC analysis calculated the energy that is consumed or released from a sample to provide endothermal and exothermic processes with quantitative and qualitative data. The energy was measured as J/g.

3.1 Experimental Design for synthesis of chitosan nanoparticles

Box-Behnken design (BBD) is applied through a computerized technique to evaluate the significance for the Ropinirole loaded chitosan nanoparticles formulation. Design-Expert® software by Stat-Ease; Inc, USA was used for the optimization of formula. Chitosan, TPP, RPM were selected as independent variable factors for Ropinirole loaded chitosan nanoparticles. The particle-size and Polydispersity index (PDI) were the responses for formulation. The software generated 15 runs (refer Table **2**) to attain the desired formula. The range of these factors and responses are shown in Table **1**.

Table 1: *Independent variables with their level and dependent variables with their constraints in Box-Behnken Design for Ropinirole loaded chitosan nanoparticles*

Name	Goal	Lower Limit	Upper Limit	Lower Weight	Upper Weight	Importance
A: Chitosan	is in range	0.05	0.4	1	1	3
B: TPP (1%)	is in range	500	1500	1	1	3
C:RPM	is in range	200	1200	1	1	3
Particle size	minimize	100	250	1	1	3
PDI	is in range	0.4	0.5	1	1	3

3.2 Preparation of optimized chitosan Nanoparticles

Various concentrations (0.4%, 0.225%, 0.05%) of chitosan solution were prepared by diluting the stock solution 0.5% w/w of stock solution using 1% of Acetic acid (15). 1% TPP solution of varying amounts was added as indicated by per Box-Behnken design.

Chitosan nanoparticles were obtained as a result of the ionic cross-linking reaction of chitosan with TPP as described in literatures.

Briefly, 20 ml of chitosan solution (0.06mg/ml in 1% acetic acid) and TPP solution (10mg/ml) was prepared in ultra purified water. Further 800 uL of 1% of TPP was added slowly to 20 ml of the above chitosan solution under magnetic stirring at 200 rpm. Nanoparticles were obtained by the interaction of chitosan solution with TPP. The resulting nanoparticles were used for further studies (16).

3.3 Preparation of Ropinirole loaded chitosan nanoparticles.

Ropinirole-loaded chitosan nanoparticles were prepared by the cross-linking method. Approximately 3ml of Ropinirole (2mg/ml concentration) mixed with 20 ml of chitosan solution (0.06 mg/ml). Further 800 uL of 1% of TPP is added slowly to the above drug-polymer mixture under magnetic stirring at 200 rpm. Finally, nanoparticles were collected and used for further characterization techniques (17).

3.4 Evaluation of Ropinirole loaded chitosan nanoparticles.

3.4.1 Particle Size, Poly dispersity Index:

Particle size and PDI of the formulations were determined using DLS method (Zeta sizer, Malvern, UK). Sufficiently diluted samples were introduced into disposable sizing cuvette, filled at a depth of 1 cm and measurements were carried out at 25±1°C with light scattering measured at right angles.

3.4.2. Drug entrapment efficiency

Using the ultracentrifugation method, it was possible to calculate the Nanoparticles Entrapment Efficiency (EE) of Ropinirole by calculating the quantity of drugs that was not entrapped. Centrifuging formulations at 15000 rpm for 25 minutes at 4°C were used to measure the EE. In order to estimate the amount of free drug in the formulation, the supernatant was collected, diluted with a suitable solvent, and subjected to UV-Visible spectroscopy analysis at 250nm (18).

3.4.3. Drug release studies from Chitosan nanoparticles

Chitosan nanoparticles dispersion of 3ml, was added into a pre-soaked dialysis kit (Pur-A-Lyzer™ Mini Dialysis Kit, Sigma Aldrich) of 14KD in 80ml simulated nasal fluid (SNF) maintained at 37±0.5°C in a 100 ml beaker. The setup was kept in agitation at 50 rpm on a magnetic stirrer with temperature control. Samples (3ml) were withdrawn at specific time intervals and measured the drug concentration using a UV-Visible spectrophotometer (Shimadzu 1800, Japan) at 250nm. Equal volume of SNF was replaced after each withdrawal(19).

3.4.4 Drug release kinetics

Preclinical drug development is dependent on data on drug release under physiologically condition simulations, which will also be the foundation for regulatory approvals and assessments of drug formulations. It is becoming more and more common to predict the in vivo release of drugs using in vitro techniques for nano formulations. In addition to helping with formulation development and controlled drug release systems, mathematical models can also be used to predict drug release mechanisms. Complexity exists in both the dosage forms for NPs and the evaluation of drug release. As a result, it can be said that the rational development of controlled release formulations involves using in vitro drug release data to forecast and characterise drug substances' in vivo performance (20).

The models are Korsmeyer-Peppas model, Higuchi Model, First order Release Kinetics Model, Zero-order Release Kinetics Model.

4.Results

FT-IR spectra

FT-IR findings predict possible interactions among drug samples and excipients in formulation. Characteristic peaks of Ropinirole, chitosan, TPP and ropinirole-chitosan was observed (Figure 1). In case of Ropinirole, stretch of conjugated aldehyde C=O was observed at 1701.88 cm^{-1}, C-H stretch was observed at 1390.06, 1455.03 and 1759.09 cm^{-1} & Amine N-H stretch were observed at 2983.53, 2969.45 and 3070.06 cm^{-1}. In case of Chitosan, alcoholic OH group stretches were observed at 3626.48, 3687.42 and 3733.08 cm^{-1}, Gama-lactam C=O stretch was observed at 1644.47 cm^{-1}, C-H stretch and bending were observed at 892.81, 1373.78 and 1416.50 cm^{-1}, 1° & 2° N-H stretch was observed at 2870.87 and 3283.83 cm^{-1} & C-O-C bridge stretch was observed at 1149.34 cm^{-1}. In case of TPP, P = O stretching, symmetric and antisymmetric stretching vibrations in PO_2 group, symmetric and antisymmetric stretching vibrations in PO_3 group, antisymmetric stretching of the P-O-P bridge were found to be 1209.50, 1126.72, 1.95.64 and 885.35 respectively. In case of Ropinirole-chitosan, C=O stretching was observed at 1702.17 and 1613.33 cm^{-1}, C-H stretch, and bending was observed at 1389.81, 1455.06, 1759.10, 878.84, 1389.81 and 1411.32 cm^{-1} & amine N-H stretch observed at 2938.04, 2969.49 and 3070.92 cm^{-1}.

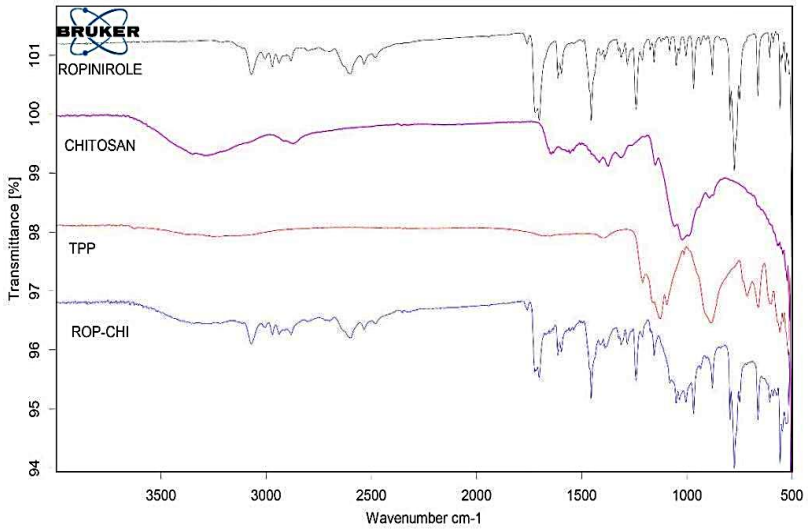

Figure 1: *FT-IR spectrum overlay of polymers and compound*

Differential Scanning Calorimetry (DSC)

DSC thermograms of Ropinirole showed sharp endothermic peak at 254.22°C (**Error! Reference source not found.**s). The DSC curve of Chitosan showed endothermic at 128.32°C and exothermic at 307.79°C (**Error! Reference source not found.**s). DSC thermographs of TPP showed endothermic at 125.72°C (**Error! Reference source not found.**s). Figure 2 shows DSC thermographs of Ropinirole - chitosan exhibited peak at 247.06°C.

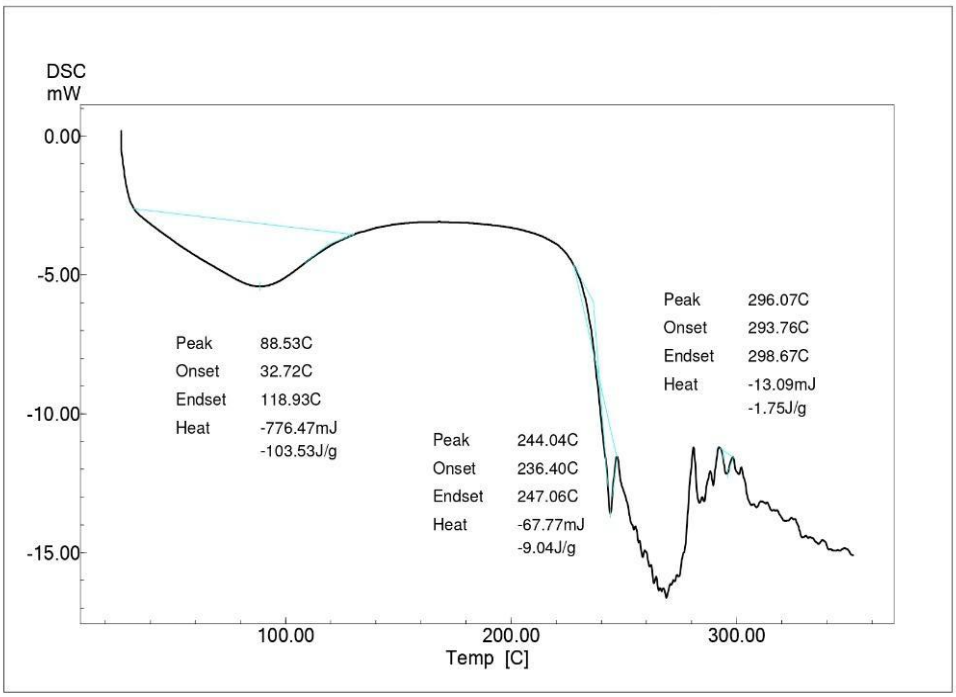

Figure 2: *DSC thermogram of Ropinirole - chitosan*

Mathematical models for design of experiments

Based on the factors assessed during screening trials, three factors (chitosan, TPP and RPM) were selected for formulation optimization of Ropinirole loaded chitosan through BBD using Design Expert software.

The BBD had generated 15 trial runs and the responses generated is displayed in Table **2.**

Table **2**.

Table 2: *BBD with observed responses for optimization of Ropinirole loaded chitosan nanoparticles*

		Factor 1	Factor 2	Factor 3	Response 1	Response 2
Std	**Run**	**A: Chitosan %**	**B: TPP (1%) µL**	**C:RPM**	**Particle size nm**	**PDI**
9	1	0.225	500	200	777.3	0.384
15	2	0.225	1000	700	441.3	0.483
1	3	0.05	500	700	129.3	0.546
12	4	0.225	1500	1200	233.9	0.444
7	5	0.05	1000	1200	335.6	0.625
11	6	0.225	500	1200	634.1	0.39
13	7	0.225	1000	700	416.2	0.428
14	8	0.225	1000	700	419.9	0.454
10	9	0.225	1500	200	364.2	0.486
2	10	0.4	500	700	1512	0.471
4	11	0.4	1500	700	821.5	0.61
6	12	0.4	1000	200	1476	0.556
5	13	0.05	1000	200	-	-
8	14	0.4	1000	1200	964.2	0.521
3	15	0.05	1500	700	-	-

ANOVA results determine significant factors depending on the p value. The factors: chitosan, TPP and RPM were found significant since it displayed p value less than 0.05 (Table 3).

4.2. ANOVA results

Analysis of Response 1: Particle size

Table 3: *ANOVA results for particle size by Box- Behnken Design*

Source	Sum of Squares	df	Mean Square	F-value	p-value	
Model	2.344E+06	9	2.604E+05	416.03	0.0002	significant
A-Chitosan	7.368E+05	1	7.368E+05	1177.09	< 0.0001	
B-TPP (1%)	1.833E+05	1	1.833E+05	292.78	0.0004	
C-RPM	17535.34	1	17535.34	28.02	0.0132	
AB	42682.65	1	42682.65	68.19	0.0037	
AC	70916.86	1	70916.86	113.30	0.0018	
BC	41.60	1	41.60	0.0665	0.8132	
A^2	79677.66	1	79677.66	127.30	0.0015	
B^2	38.22	1	38.22	0.0611	0.8208	
C^2	15003.68	1	15003.68	23.97	0.0163	
Residual	1877.73	3	625.91			
Lack of Fit	1510.51	1	1510.51	8.23	0.1031	not significant
Pure Error	367.22	2	183.61			
Cor Total	2.345E+06	12				

These rows were ignored for this analysis: 15, 13 due to inconsistencies and coagulation of particles. Factor coding is '**Coded'**.
The Sum of squares is **Type III - Partial**

The **Model F-value** of 416.03 implies the model is significant. There is only a 0.02% chance that an F-value this large could occur due to noise.

P-values less than 0.0500 indicated model terms are significant. In this case A, B, C, AB, AC, A^2, C^2 are significant model terms. Values greater than 0.1000 indicate the model terms are not significant. If there are many insignificant model terms (not counting those required to support hierarchy), model reduction may improve your model.

The **Lack of Fit F-value** of 8.23 implies the Lack of Fit is not significant relative to the pure error. There is a 10.31% chance that a Lack of Fit F-value this large could occur due to noise. A non-significant lack of fit is good as we want the model to fit.

Final Linear Equation in Terms of Coded Factors are:

Particle size = 425.80 + 525.62A - 195.39B - 60.44C - 157.79AB - 203.39AC + 3.22BC + 203.71A^2 + 3.68B^2 + 72.90C^2

The equation in terms of coded factors can be used to make predictions about the response for given levels of each factor. By default, the high levels of the factors are coded as +1 and the low levels are coded as -1. The coded equation is useful for identifying the relative impact of the factors by comparing the factor coefficients.

Graphical Representation

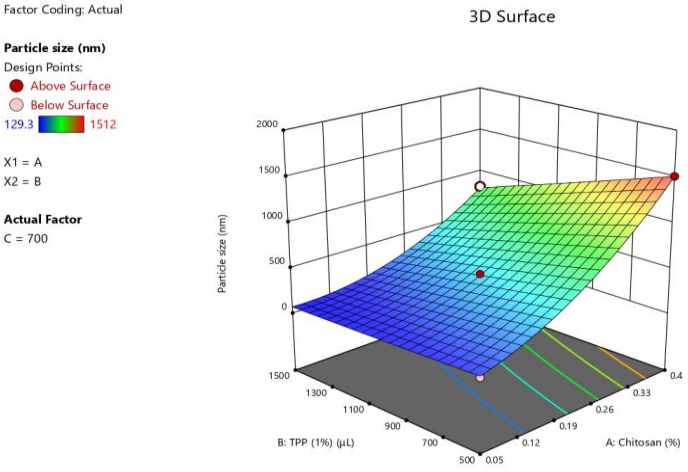

Figure 3: *3D surface plot demonstrating the effect of factors on the particle size*

Analysis of Response 2: PDI

Table 4: *ANOVA results for PDI by Box- Behnken*

Source	Sum of Squares	df	Mean Square	F-value	p-value	
Model	0.0675	9	0.0075	9.37	0.0459	significant
A-Chitosan	0.0017	1	0.0017	2.12	0.2411	
B-TPP (1%)	0.0098	1	0.0098	12.18	0.0398	
C-RPM	0.0000	1	0.0000	0.0510	0.8358	
AB	0.0006	1	0.0006	0.7196	0.4586	
AC	0.0007	1	0.0007	0.9144	0.4095	
BC	0.0006	1	0.0006	0.7194	0.4587	
A^2	0.0296	1	0.0296	37.02	0.0089	
B^2	0.0011	1	0.0011	1.35	0.3290	
C^2	0.0003	1	0.0003	0.3127	0.6151	
Residual	0.0024	3	0.0008			
Lack of Fit	0.0009	1	0.0009	1.17	0.3919	not significant
Pure Error	0.0015	2	0.0008			
Cor Total	0.0699	12				

These rows were ignored for this analysis: 15, 13
Factor coding is **Coded**.
Sum of squares is **Type III - Partial**

The **Model F-value** of 9.37 implies the model is significant. There is only a 4.59% chance that an F-value this large could occur due to noise.
P-values less than 0.0500 indicate model terms are significant. In this case B, A^2 are significant model terms. Values greater than 0.1000 indicate the model terms are not significant. If there are many insignificant model terms (not counting those required to support hierarchy), model reduction may improve your model.

The **Lack of Fit F-value** of 1.17 implies the Lack of Fit is not significant relative to the pure error. There is a 39.19% chance that a Lack of Fit F-value this large could occur due to noise. A non-significant lack of fit is good as we want the model to fit.

Final Linear Equation in Terms of Coded Factors:

PDI = 0.4550 – 0.0253A + 0.0451B – 0.0029C + 0.0183B – 0.0207AC – 0.0120BC + 0.1243A^2 – 0.0196B^2 – 0.0094C^2

The equation in terms of coded factors can be used to make predictions about the response for given levels of each factor. By default, the high levels of the factors are coded as +1 and the low levels are coded as -1. The coded equation is useful for identifying the relative impact of the factors by comparing the factor coefficients.

Graphical Representation

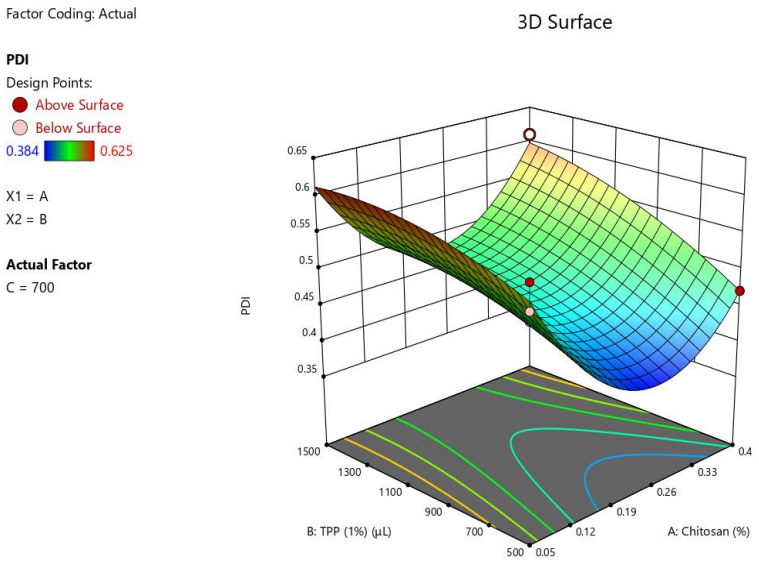

Figure 4: *3D graphs for demonstrating relationship between various factors on PDI*

Number of solutions obtained using Design of Experiment (DoE)

Using three factors that is Chitosan, TPP and RPM, 68 solutions obtained by Design of Experiment (DoE) among which the one with highest desirability was chosen. The solution is shown in that Table 5.

Responses demonstrating the relationship between factor A and B on desirability, particle size and PDI (Figure 5**).**

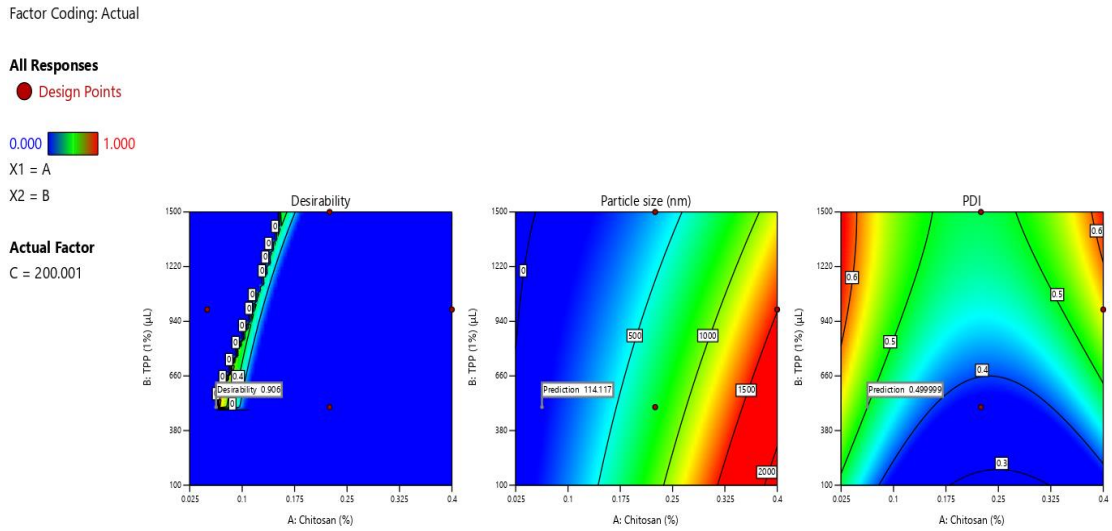

Figure 5: *Demonstrating relationship between factor A and B on desirability, particle size and PDI of all responses*

Table 5: *Predicted vs obtained mean of particle size and PDI*

Solution 1 of 62 Response	Predicted Mean	Predicted Median	Observed	Std Dev	n	SE Pred	95% PI low	Data Mean	95% PI high
Particle size	114.117	114.117	**139.4**	25.0182	1	48.4588	-40.1006	140.2	268.334
PDI	0.499999	0.499999	**0.328**	0.028297	1	0.0548098	0.32557	0.328	0.674428

Evaluation of Ropinirole loaded Chitosan Nanoparticles

Evaluation of particle-size, PDI & zeta-potential

Bare chitosan nanoparticles displayed average particle size and PDI of 139.4 nm and 0.328. Zeta potential of bare chitosan nanoparticle was found to be 20.0 mV.

Ropinirole loaded chitosan nanoparticles displayed an average particle-size & PDI of 156.7 nm and 0.241. The zeta potential of Ropinirole loaded chitosan nanoparticles was found to be 11 mV.

Drug entrapment efficiency

Drug Entrapment efficiency for chitosan nanoparticle formulation was found to be 91%.

Drug Release Kinetics

Different invitro kinetics models were performed and based on the R^2 value the best suitable model for the invitro data was found to be the first-order model as in Table 6 and the **Error! Reference s ource not found.** shows the drug release pattern from the chitosan nanoparticles.

Table 6: *Drug release kinetic modelling data of drug release*

Plot	Slope	R2 value	n	Drug release Mechanism
0 order	6.8255	0.9159		
1 order	-0.0681	**0.9917**		First order drug release
Higuchi	0.0347	**0.9818**		Fickian Diffusion controlled Drug release
Kosmeyer Peppas	1.2505	0.9584	1.1281	

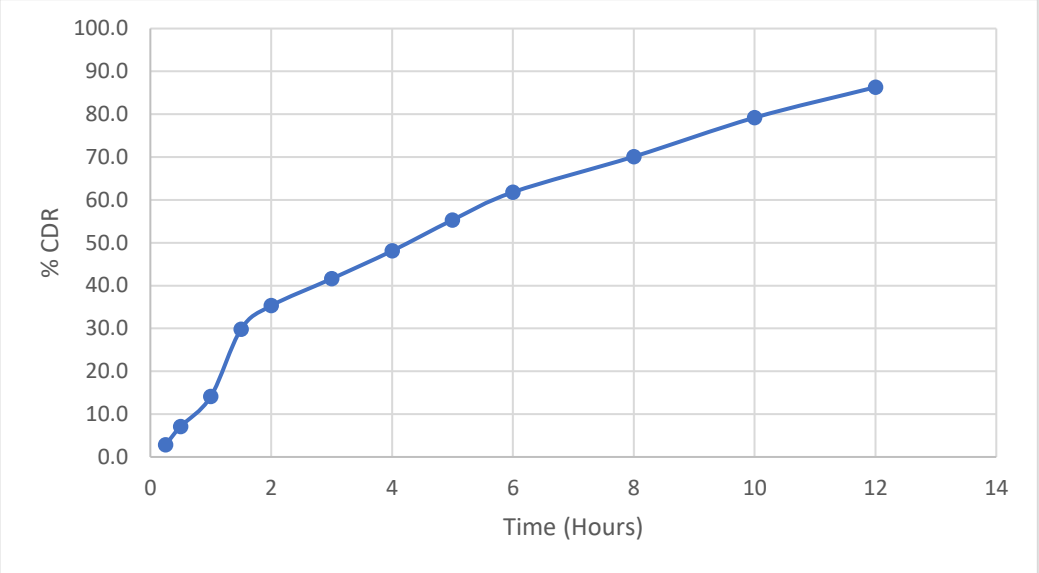

Figure 6: *Release of Ropinirole from chitosan nanoparticles in Physiological pH*

5. Discussion

5.1. Characterization of Ropinirole loaded Chitosan Nanoparticles

5.1.1. FT- IR spectra

The FTIR results show that the Ropinirole has no chemical bond with the polymer used in the preparation. So, the drug is compatible with polymer.

5.1.2. Differential Scanning Calorimetry (DSC)

DSC thermogram of optimized formulation of Ropinirole and Ropinirole loaded chitosan nanoparticle exhibited a decline in melting point of drug which might be due to a reduction in crystalline nature of compounds.

5.2 Formulation studies

5.2.1. Mathematical models for the designing of experiments

Design Expert software was utilized for illustrating the response surface methodology (RSM) by combining the values. A type of second-order design known as Box Behnken Design (BBD) is based on incomplete factorial designs with three levels. For the optimization of the synthesized NS, a Box Behnken (three factors at three different levels) experimental design was implied. A three-part design with one factor set to zero level and the other two consisting of two fully levelled factors. The second-order polynomial model was studied using Design Expert ® (13.0.5, Stat-Ease Inc., Minneapolis, MN, USA), which was utilized to analyze the quadratic response surfaces. Optimization using minimal experimental trial runs can be carried out using BBD. In the current study, BBD was an ideal design chosen for optimization of Ropinirole loaded chitosan nanoparticles, and 15 runs were generated (Table 3).

5.2.1.1. ANOVA for Ropinirole loaded Chitosan Nanoparticles

Particle size

As per Table 3, the F value of 416.03 and p-value of 0.0002 indicate the model's significance. The final regression equation, after including the values of all coefficients is provided in the result section. The table illustrates the outcome of individual variables and the interactional effects on particle size.

PDI

As per Table 4, the F value of 9.37 and p-value of 0.0459 indicate the model's significance. The final regression equation, after including values of all coefficients is provided in the result section. The table illustrates the outcome of individual variables and the interactional effects on particle size.

3D graphs for demonstrating the relationship between various factors A, B and C on particle size and PDI of Ropinirole loaded chitosan nanoparticles formulation.

3D graphs give a 3D view on the effect of each factor on the responses (Figure 3 and Figure 4).

5.3. Evaluation of Chitosan Nanoparticles

5.3.1. Particle size and PDI

As the particle size of the optimized formulation is in nano size range as per the requirement which could be able to penetrate through the mucus layer and pass through the BBB and reach the target site.

5.3.2. Zeta potential

Zeta potential of final optimized formulations of bare chitosan nanoparticle and Ropinirole loaded chitosan nanoparticles are found to be -23.0mV and -27.6mV respectively. Zeta potential of ± 30mV is ideal. It indicates stability of the preparation.

A negative zeta potential for the ropinirole loaded chitosan nanoparticle may result in repulsion from the negatively charged mucus membrane. This repulsion can potentially limit the adhesion and interaction of the nanoparticles with the mucosal surface, affecting their penetrability and bioavailability. However, by looking the other factors, such as the composition, surface modification of the nanoparticles and also size less than 200nm, can also influence their behaviour in nasal delivery as chitosan itself is known to have mucoadhesive properties, which can help promote interaction with the mucus membrane and improve drug absorption (21).

Drug Release Kinetics:

The release of pharmaceuticals from an insoluble matrix is described by Higuchi's mode as the square root of a time-dependent process based on Fickian diffusion (22,23). Based on the correlation coefficient values of the various models, the model that best fits the release data was chosen. Higher R^2 values (0.98) in the Higuchi model supported the findings that drug release from NPs was diffusion-controlled (17).

Conclusion

The development of ropinirole-loaded chitosan nanoparticles for intranasal delivery in Parkinson's disease using the Box-Behnken design offers a promising approach for enhanced drug delivery to the brain. Parkinson's disease is a prevalent neurodegenerative disorder, and the intranasal route provides several advantages, such as needle-free administration, non-invasiveness, and direct delivery to the central nervous system. Overall, the development of ropinirole-loaded chitosan nanoparticles for intranasal delivery holds promise in improving the targeted delivery of drugs to the brain for the treatment of Parkinson's disease. This approach may enhance drug concentration in the brain, bypass the blood-brain barrier, and reduce dosing frequency while minimizing systemic side effects. Further studies and in vivo evaluations are necessary to validate the potential of these nanoparticles as an effective treatment strategy for Parkinson's disease.

Conflicts of Interest: The author declares no conflict of interest.

References:

1. Marras C, Beck JC, Bower JH, Roberts E, Ritz B, Ross GW, et al. Prevalence of Parkinson's disease across North America. NPJ Parkinsons Dis [Internet]. 2018 Dec 1 [cited 2023 May 11];4(1). Available from: https://www.parkinson.org/understanding-parkinsons/statistics
2. V AN, George P, L DA. Application of 32 Factorial D-Optimal Design in Formulation of Porous Osmotic Pump Tablets of Ropinirole; An Anti-Parkinson's Agent. Journal of Young Pharmacists. 2017 Jan 10;9(1):87–93.
3. Nashatizadeh M, Lyons KE, Pahwa R. A review of ropinirole prolonged release in Parkinson's disease. Clin Interv Aging [Internet]. 2009 [cited 2023 May 11];4(1):179–86. Available from: https://pubmed.ncbi.nlm.nih.gov/19503779/
4. Shill HA, Stacy M. Update on ropinirole in the treatment of Parkinson's disease. Neuro psychiatr Dis Treat [Internet]. 2009 [cited 2023 May 11]; 5(1): 33. Available from: /pmc/articles/PMC2695212/
5. V A, Cutinho LI, Mourya P, Maxwell A, Thomas G, Rajput BS. Approaches for encephalic drug delivery using nanomaterials: The current status. Brain Res Bull. 2020 Feb;155:184–90.
6. Jadhav K, Gambhire M, Shaikh I, Kadam V, Pisal S. Nasal Drug Delivery System-Factors Affecting and Applications. Curr Drug ther. 2008 Apr 18;2(1):27–38.
7. Bypassing the blood-brain barrier to deliver therapeutic agents to the brain and spinal cord | Request PDF [Internet]. [cited 2023 May 11]. Available from: https://www.researchgate.net/publication/284695725_Bypassing_the_blood-brain_barrier_to_deliver_therapeutic_agents_to_the_brain_and_spinal_cord
8. Liu XF, Fawcett JR, Thorne RG, DeFor TA, Frey WH. Intranasal administration of insulin-like growth factor-I bypasses the blood–brain barrier and protects against focal cerebral ischemic damage. J Neurol Sci. 2001 Jun 15;187(1–2):91–7.
9. Chow HHS, Chen Z, Matsuura GT. Direct transport of cocaine from the nasal cavity to the brain following intranasal cocaine administration in rats. J Pharm Sci [Internet]. 1999 Aug 1 [cited 2023 May 11];88(8):754–8. Available from:

https://onlinelibrary.wiley.com/doi/full/10.1021/js9900295
10. Bhattamisra SK, Shak AT, Xi LW, Safian NH, Choudhury H, Lim WM, et al. Nose to brain delivery of rotigotine loaded chitosan nanoparticles in human SH-SY5Y neuro blastoma cells and animal model of Parkinson's disease. Int J Pharm. 2020 Apr;579:119148.
11. Kaur S, Manhas P, Swami A, Bhandari R, Sharma KK, Jain R, et al. Bioengineered PLGA-chitosan nanoparticles for brain targeted intranasal delivery of antiepileptic TRH analogues. Chemical Engineering Journal. 2018 Aug; 346:630–9.
12. Sridhar V, Gaud R, Bajaj A, Wairkar S. Pharmacokinetics and pharmacodynamics of intranasally administered selegiline nano particles with improved brain delivery in Parkinson's disease. Nanomedicine. 2018 Nov;14(8):2609–18.
13. Lee D, Minko T. Nanotherapeutics for Nose-to-Brain Drug Delivery: An Approach to Bypass the Blood Brain Barrier. Pharmaceutics. 2021 Nov 30;13(12):2049.
14. Yu S, Xu X, Feng J, Liu M, Hu K. Chitosan and chitosan coating nanoparticles for the treatment of brain disease. Int J Pharm. 2019 Apr;560:282–93.
15. Tanasale MFJDP, Bijang CM, Rumpakwara E. Preparation of Chitosan with Various Molecular Weight and Its Effect on Depolymerization of Chitosan with Hydrogen Peroxide using Conventional Technique. Int J Chemtech Res. 2019;12(01):112–20.
16. Balde A, Hasan A, Joshi I, Nazeer RA. Preparation and optimization of chitosan nanoparticles from discarded squilla (Carinosquilla multicarinata) shells for the delivery of anti-inflammatory drug: Diclofenac. J Air Waste Manage Assoc. 2020 Dec 1;70(12):1227–35.
17. Jafarieh O, Md S, Ali M, Baboota S, Sahni JK, Kumari B, et al. Design, characterization, and evaluation of intranasal delivery of ropinirole-loaded mucoadhesive nanoparticles for brain targeting. Drug Dev Ind Pharm. 2015 Oct 3;41(10):1674–81.
18. Rinaldi F, Hanieh P, Chan L, Angeloni L, Passeri D, Rossi M, et al. Chitosan Glutamate-Coated Niosomes: A Proposal for Nose-to-Brain Delivery. Pharmaceutics. 2018 Mar 22;10(2):38.
19. Galgatte UC, Kumbhar AB, Chaudhari PD. Development of in situ gel for nasal delivery: design, optimization, in vitro and in vivo evaluation. Drug Deliv. 2014 Feb 5;21(1):62–73.
20. Herdiana Y, Wathoni N, Shamsuddin S, Muchtaridi M. Drug release study of the chitosan-based nanoparticles. Heliyon. 2022 Jan;8(1):e08674.
21. Mikušová V, Mikuš P. Advances in Chitosan-Based Nanoparticles for Drug Delivery. Int J Mol Sci. 2021 Sep 6;22(17):9652.
22. Paul DR. Elaborations on the Higuchi model for drug delivery. Int J Pharm. 2011 Oct;418(1):13–7.
23. Bayer IS. Controlled Drug Release from Nano engineered Polysaccharides. Pharmaceutics. 2023 Apr 28;15(5):1364.